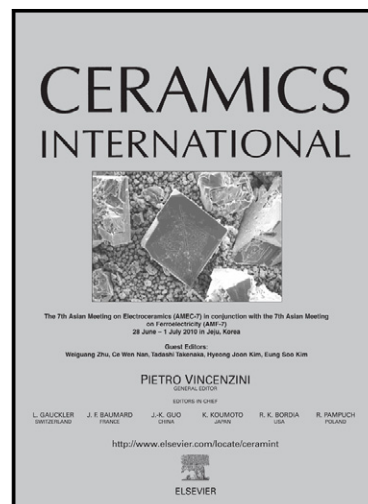


Author's Accepted Manuscript

Mechanically induced self-propagating reaction of vanadium carbonitride

M.A. Roldán, M.D. Alcalá, C. Real



www.elsevier.com/locate/ceramint

PII: S0272-8842(14)01937-3
DOI: <http://dx.doi.org/10.1016/j.ceramint.2014.12.016>
Reference: CERI9617

To appear in: *Ceramics International*

Received date: 6 November 2014
Revised date: 1 December 2014
Accepted date: 2 December 2014

Cite this article as: M.A. Roldán, M.D. Alcalá, C. Real, Mechanically induced self-propagating reaction of vanadium carbonitride, *Ceramics International*, <http://dx.doi.org/10.1016/j.ceramint.2014.12.016>

This is a PDF file of an unedited manuscript that has been accepted for publication. As a service to our customers we are providing this early version of the manuscript. The manuscript will undergo copyediting, typesetting, and review of the resulting galley proof before it is published in its final citable form. Please note that during the production process errors may be discovered which could affect the content, and all legal disclaimers that apply to the journal pertain.

MECHANICALLY INDUCED SELF-PROPAGATING REACTION OF VANADIUM CARBONITRIDE

M.A. Roldán, M.D. Alcalá, C. Real*

Instituto Ciencias de Materiales de Sevilla CSIC-US, Av. Américo Vespucio nº49, 41092-Sevilla (Spain)

*Corresponding autor.

Abstract

Vanadium carbonitrides (VC_xN_{1-x}) were prepared via mechanosynthesis from mixtures of elemental vanadium and carbon with different V/C atomic ratios under a nitrogen atmosphere using a high-energy ball mill. We obtained the full composition range of carbonitrides at room temperature. The products were characterized using X-ray diffraction, scanning electron microscopy and electron energy loss spectroscopy. The results showed particle-sized products with high sinterability and very high microhardness.

Keywords

Mechanosynthesis; Vanadium carbonitride; EELS; Microhardness

Introduction

Transition metal carbonitrides are important materials because of their unique and outstanding combination of physical properties, such as high melting points, high hardnesses, good thermal and chemical stabilities, and excellent electrical and thermal conductivities, among others. These properties make carbonitrides useful materials for a wide range of applications, such as coatings and cutting tools. Furthermore, carbonitrides are widely being used in the preparation of advanced engineering ceramic-based composites that are employed in several applications in key high-level technologies¹⁻³.

Currently, the most common synthesis methods for producing carbonitrides are chemical vapor deposition from organometallic precursors⁴⁻⁹, thermal diffusion^{3,10}, solid-state reactions from precursor oxides and carbides¹¹⁻¹³, and self-sustaining high-temperature synthesis from vanadium carbide¹⁴. This last procedure appears to be a good alternative to the classic metallurgic methods for synthesizing borides, carbides, nitrides and carbonitrides¹⁵⁻²³. It has been established that the physical and chemical properties of these solid solutions depend on their compositions (C/N ratio)^{3,24-25}; however, the aforementioned methods do not allow for the synthesis of these materials

over the entire composition range. Our group has previously reported²⁶⁻²⁸ that mechanical synthesis methods provide good results in the synthesis of these types of compounds, affording particles with nanometric sizes. There are examples in the literature of the synthesis of VC using mechanical processes²⁹⁻³⁰, as well as examples of other carbonitrides synthesized using self-propagating or combustion reactions induced by milling^{26-27,31-32}. In the present paper, we synthesize vanadium carbonitride from its constituent elements using reactive milling. Reactive milling is an easier, faster and more economical process than the previous methods. The microstructural characterization and hardnesses of the final products are also presented.

Experimental

Graphite powder (<270 mesh, Fe≤0.4%, Merck), vanadium (99.5% purity, <100 mesh, Aldrich) and nitrogen (99.9%; H₂O≤3 ppm, O₂ ≤2 ppm and C_nH_m ≤5 ppm; Air Liquide) were used in this work.

Different C-V powder mixtures were milled under 11 bars of high-purity nitrogen gas using a modified planetary ball mill (Fritsch model Pulverisette 7) at a rotation rate of 700 rpm for both the rotation of the supporting disc and the superimposed rotation in the direction opposite to the vial. Six tempered steel balls and 5 g of reactive powder (C-V) were placed in a tempered steel vial (67Rc) for each milling experiment. The volume of the vial was 45 ml. The diameter and weight of the balls were 15 mm and 13.85 g, respectively. The powder-to-ball mass ratio (PBR) was 1/16. The vial was purged with nitrogen gas several times, and then the desired nitrogen pressure (11 bars) was achieved prior to milling. The vial was permanently connected to the gas cylinder during the milling experiments through a rotary valve and a flexible polyamide tube. The pressure was continuously monitored using a SMC solenoid valve (model EVT307-5DO-01F-Q, SMC) connected to an ADAM-4000 series data acquisition system (Esis Pty Ltd.). The self-sustaining reaction inside the vial was detected from the time–pressure value, which was monitored during milling. This record exhibited a peak when the ignition occurred due to the heat generated by the highly exothermic reaction.

X-ray powder diffraction patterns were recorded using a Philips X'Pert Pro diffractometer equipped with a Θ/Θ goniometer using Cu K α radiation (40 kV, 40 mA), a secondary K β filter, and an X'Celerator detector. The diffraction patterns were scanned from 10° to 90° (2 Θ) at a scan rate of 0.42° min⁻¹. Silicon powder (NIST) was

used to correct the XRD peak shifts. The lattice parameter, a , of the VC_xN_{1-x} phases was calculated from the entire set of peaks in the XRD pattern using the Lapods computer program assuming a cubic symmetry. The average crystalline size of the powder was estimated using the Scherrer equation.

The iron contamination in the milled samples was determined using Fe^{2+} permanganometry.

The formation of carbonitrides was also studied using a high-resolution transmission electron microscope (Philips CM200, Eindhoven) equipped with a super twin objective lens and operated at 200 kV with a LaB_6 filament. The TEM was equipped with a parallel electron energy loss (EELS) spectrometer (Model 766-2K, Gatan, München, Germany). The N, C and V core-loss edges were recorded in the diffraction mode with a camera length of 470 mm using a 2-mm spectrometer; the entrance aperture yielded an energy resolution at the zero-loss peak of 1.4 eV. Spectra were recorded for dark current and channel-to-channel gain variation. After subtraction of the background using a standard power-law function, the spectra were deconvoluted for plural scattering with the Fourier-ratio method and normalized to the jump. All of these treatments were performed within the EL/P program (Gatan).

Microstructural observations were conducted using scanning electron microscopy (SEM model JSM 5400 Jeol). The SEM images were recorded at 30 kV. For the SEM observations, the powdered samples were dispersed in ethanol and supported on a metallic grid.

The different samples were sintered using a pressureless process. The samples were first shaped (green bodies) and then sintered at high temperature. The forming process was performed using cold isostatic pressing at 2000 bars for 5 min. The green bodies were sintered at 1750°C for 60 min (heating rate of 5°C/min, free cooling) under an inert atmosphere (helium gas, $H_2O \leq 3$ ppm, $O_2 \leq 2$ ppm and $CnHm \leq 0.5$ ppm, Air Liquide) in a horizontal furnace (Thermolyne Type 59300 model no. F-59340-CM).

Vickers microhardness measurements (FM-700, Future-Tech, Hardness tester) were conducted on cross sections of pellets under a load of 1 kgf for 15 s. An average hardness was calculated from 20 indents per specimen.

Results and discussion

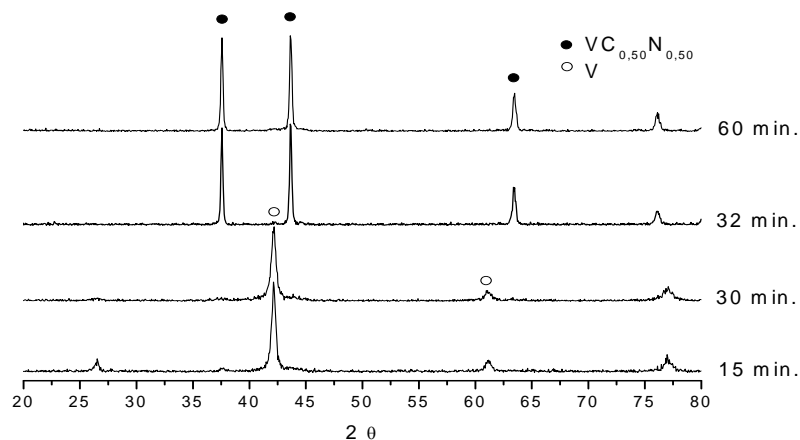
Table I presents the different compositions prepared via mechanosynthesis and the required preparation times:

Table I. Milling times of the final vanadium carbonitrides.

x ($\text{VC}_x\text{N}_{1-x}$)	0.00	0.25	0.30	0.40	0.50	0.55	0.60	0.75	0.85	0.95	1.00
Combustion Time (min)	--	--	120	61	32	42	53	56	61	55	--
Milling Time (min)	480	300	150	90	60	70	80	80	90	80	240

We can observe two different synthesis mechanisms: the combustion induced by the milling process mechanism (self-auto-propagating reaction), which corresponds to the carbonitrides with compositions of $x=0.3$ to 0.95 , and the diffusion mechanism, which corresponds to the compositions ($x=0.25$) and ($x=0$ and 1).

Fig. 1 shows the X-ray diffraction patterns for the composition $\text{VC}_{0.5}\text{N}_{0.5}$ with different milling times, which was obtained via the combustion mechanism, as an example. The diffraction peaks of vanadium broaden as the milling time increases (prior to 30 min, which is the ignition time); after 32 min of the SHS process, only the diffraction peaks of the carbonitride are observed. After the combustion reaction, the milling continues for another 30 minutes to ensure that the reaction is complete and to homogenize the newly formed material. As shown in Fig. 1, the composition of the sample does not change during this time.

**Fig. 1.** X-Ray diffraction patterns of the sample with a nominal composition of $\text{VC}_{0.5}\text{N}_{0.5}$ at different milling times.

For the sample with a composition of $x=0.25$, the reaction follows a diffusion mechanism similar to that for VC and VN. Fig. 2 presents the X-ray diffraction patterns for this sample at different milling times. The analysis of the XRD patterns indicates that the V peaks broaden with increasing milling time due to the refinement of the crystallite size, the formation of defects, and microstrains in the milled samples. Furthermore, the diffraction patterns begin to exhibit peaks corresponding to vanadium carbonitride. After 3 h of milling, the VCN peaks are the most prominent peaks in the diffraction pattern. Further increasing the milling time to 5 h led to a continuous increase in the intensities of the VCN diffraction peaks; the considerable broadening of the VCN diffraction peaks suggests that this phase was obtained with a very refined microstructure and a high level of microstrains.

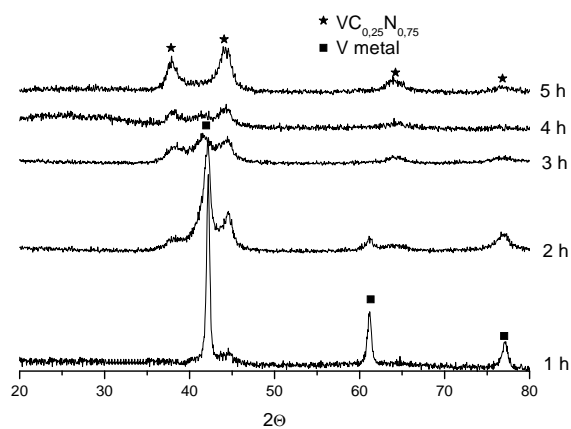


Fig. 2. X-ray diffraction patterns of the sample with a nominal composition of $VC_{0.25}N_{0.75}$ at different milling times.

The sample with a composition corresponding to $x=0.3$ is special due to a combustion reaction during the milling process, but the required ignition time is higher than the ignition time for the other compositions. Moreover, the final product is not only carbonitride because a mixture of products is obtained (VC_xN_{1-x} , V_2N and V_2C), as shown in Fig. 3.

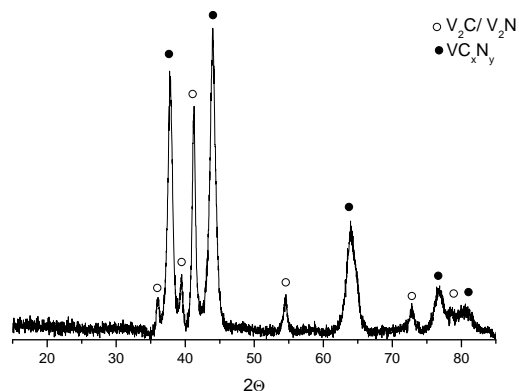


Fig. 3. X-Ray diffraction pattern of the final product of the sample with a nominal composition of $VC_{0.3}N_{0.7}$.

The literature indicates that the self-propagating reaction induced by ball milling is similar to the self-sustaining high-temperature synthesis (SHS), in which the nomenclature is the same as that proposed by Yen³³ (MSR), and it can be divided into three steps.

1. An activation period in which the particle size decreases, the number of defects increases and, in some cases, a small amount of product is formed via the diffusion process.
2. An ignition period in which a very high local temperature is reached, the reaction propagates for the whole sample and the product is formed instantly.
3. After the ignition period, a partial combustion occurs, which means that extra milling time is required to complete the reaction and to homogenize the formed product.

On the other hand, according to data in the literature^{26-27,32-37} for reactions that follow an MSR process, the condition is always an adiabatic temperature above 2000 K, and in the same family of compounds, this reaction mechanism typically occurs in a determined range of compositions. Therefore, in a review of this type of grinding-induced reaction, Takacs³⁶ commented that the high ignition time is occasionally caused by small amounts of reaction products formed via diffusion at the beginning of grinding, which inhibit the reaction as inert additives; thus, when combustion does not occur before a minimum time, the reaction proceeds via diffusion. On studies of SHS, Yeh et al.³⁸⁻⁴⁰ found that during the formation of carbonitrides of Ti, Nb and Ta, after combustion, a propagation front is generated that runs across the sample and that the

front extension decreases as the carbon content increases. In this type of reaction, nitrogen is incorporated in the second stage of the process, and as the front extension decreases, a smaller amount of nitrogen is incorporated. The maximum incorporation of nitrogen occurs for $C/N = 1$. For this reason, and taking into account that for compositions with $C/N > 0.7$, the quantity of metal available for the reaction is less, it becomes difficult to prepare samples with nitrogen-deficient compositions using this procedure. Yeh et al.¹² applied SHS to obtain vanadium carbonitride, VC_xN_{1-x} , for compositions over $x = 0.3$; within the range of $x = 0.3$ to $x = 0.7$, they observed that afterburning occurs along the sample after combustion. For $x = 0.5$, the formed carbonitride presented the highest nitridation value, and nitrogen-deficient carbonitrides were obtained for x values between 0.5 and 0.7. For $x = 0.3$, the products were a nitrogen-deficient carbonitride and V_2N because there was less C available and because V_2N is not soluble with carbide phase, and thus, the reaction does not proceed toward formation of the compound. In the case of MSR reactions, both carbon and nitrogen react together with the metal; thus, preparing nitrogen-deficient compositions is feasible using MSR reactions. These two methods are in some ways parallel, but they may also be complementary for the preparation of these materials. Our results are in good agreement with the literature^{14, 38-40}, in which the limit of $x = 0.25$ is commonly used to prepare compounds using these processes (MRS and SHS). Similarly, with the composition $x = 0.3$, the formation of other compounds is detected, as also observed for Nb, Ta, Hf and V.

The crystallite sizes of the different samples were estimated using the Scherrer equation, and these values are presented in Table II. The lattice constants of the VCN cubic unit cell were determined from the entire set of peaks in the diffraction patterns, which were recorded from 10 to 90 °2 θ for all samples. Least-squares fittings of the XRD peaks were performed using the Lapoud program.³⁷, and the results are presented in Table II.

Table II also presents the lattice parameters calculated using Vegard's law for the different compositions. The comparison of these values with the experimentally calculated values with the Lapoud program reveals some deviation, indicating that the obtained compounds are deformed and/or, in many cases, the obtained compounds are not stoichiometric, being deficient in nitrogen, as previously observed by Yeh et al.¹⁴ in their study of this family of compounds obtained using SHS.

The level of iron contamination was calculated from chemical analysis of the total iron content by titration and revealed that contamination by this metal occurred during grinding, although it never exceeded 4%. The corresponding percentages of iron and the values are included in Table II, which indicate that the samples obtained by combustion present values of approximately 1% and increase to near 4% in samples obtained by diffusion. This result and the degree of crystallinity of the obtained samples represent one of the advantages of the combustion mechanism. The combustion mechanism also has an economic advantage because of shorter milling times.

Table II. Lattice parameter (a), crystallite size, maximum strain and iron contamination of the final product.

Sample	a(Å) L. Vegard	a (Å)	DDC (nm)	Microstrains (10^{-3})	%Fe
VC _{0.25} N _{0.75}	4.1457	4.1388	8.25	1.252	3.5
VC _{0.30} N _{0.70}	4.1471	--	18.30	0.692	2.1
VC _{0.40} N _{0.60}	4.1496	4.146	163.50	0.242	0.9
VC _{0.50} N _{0.50}	4.1521	4.148	127.05	0.182	0.8
VC _{0.55} N _{0.45}	4.1536	4.143	112.65	0.153	0.8
VC _{0.60} N _{0.40}	4.1547	4.144	148.35	0.146	1.2
VC _{0.75} N _{0.25}	4.1586	4.153	157.30	0.133	0.7
VC _{0.85} N _{0.15}	4.1612	4.156	158.15	0.128	0.6
VC _{0.95} N _{0.05}	4.1638	4.158	150.00	0.137	0.7

The characterization was completed by measuring energy loss spectra in the transmission electron microscope. Fig. 4 shows the nitrogen and C K-edges for the different prepared samples. The data in the literature for such compounds, particularly titanium carbonitride⁴¹⁻⁴³, show that the carbon K-edge of a carbide is identified by two peaks centered at approximately 283 eV (π bond) and 292 eV (σ bond), in which the first is of higher intensity than the second; the free amorphous carbon is identified by a peak at 285.6 eV and a broader and higher intensity peak at 296 eV. Finally, the carbonitride presents the same peaks as the carbide, 283 eV and 292 eV, but in this case, the second peak was slightly more intense than the first peak because of the inverse relationship for the orbital occupation density involved with respect to the carbide. Figure 4 shows that

- The composition $x = 0.25$ has a spectrum with the peak at 286 eV and a higher intensity peak at 296 eV; according to the literature⁴¹⁻⁴³, this behavior indicates the presence of amorphous carbon or a nitride with the amorphous carbon on a

grain boundary. However, this composition is obtained by a diffusion mechanism, and more milling time was required. The X-ray diffraction patterns (Fig. 2) exhibit broad and asymmetric peaks with some level of microstrains. We believe that all of these results contribute to deforming and changing the appearance of the peak corresponding to the carbon K-edge.

- The composition $x = 0.3$ shows two peaks positioned at 283 eV and 293 eV, in which the first peak has a greater intensity than the second peak. This result is similar to the spectrum of a carbide according to the data from the literature, but note that in our case for this composition, we obtained a mixture of phases, carbonitride and carbide, which could explain the change in the spectrum.
- For other compositions, we obtained two peaks at 283 eV and 293 eV, in which the second peak was of higher intensity than the first, corresponding to a carbonitride.
- On the other hand, the peaks corresponding to K-edge of nitrogen increased as x decreased.

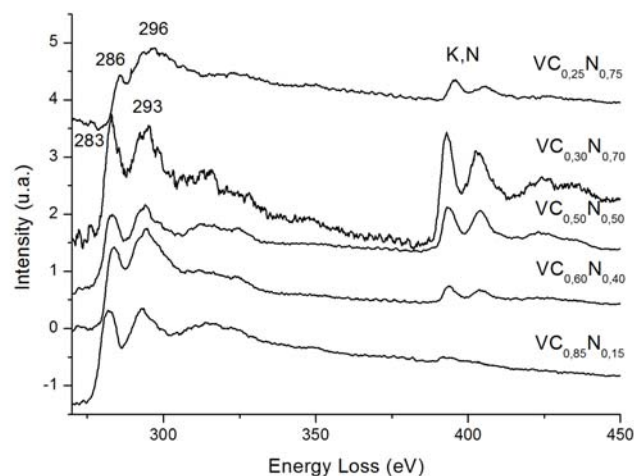


Fig. 4. EELS spectra at the C K-edge and N K-edge of the different carbonitrides prepared.

The morphology studies for the different samples are shown in Fig. 5. The composition of $x = 0.25$, which was obtained via a diffusion mechanism, exhibits great heterogeneity, and their agglomerates, which are formed by small crystallites, can range in size up to 1-2 μm . The sample with a composition of $x = 0.3$ exhibits greater heterogeneity of particles and fibers, which is reasonable because this sample is not a

single phase; it is a mixture of compounds. For the following compositions, we can observe the same morphology in the form of flakes due to the high temperatures reached during the combustion reaction.

The prepared samples were sintered to measure their microhardnesses. First, green bodies were obtained as pellets, with 400 mg of sample, by employing isostatic pressing. Then, they were sintered at 1750°C for 1 h under a helium atmosphere. The densities of the samples were measured using the Archimedes method, and the microhardness values were obtained using the equipment described in the Experimental Section; these values are shown in Table III.

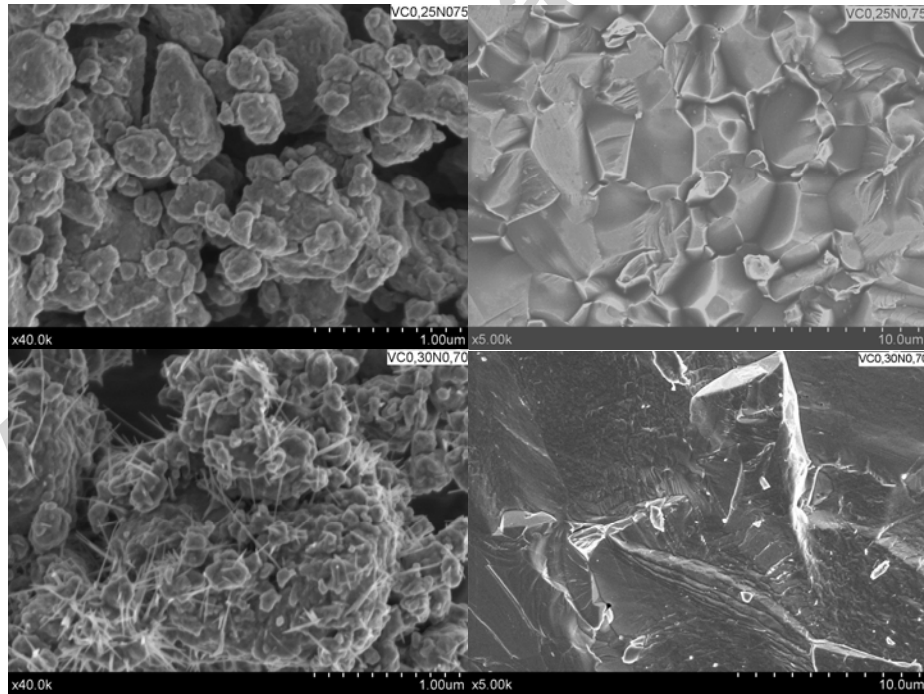
Table III. The densification and microhardnesses of the prepared carbonitrides

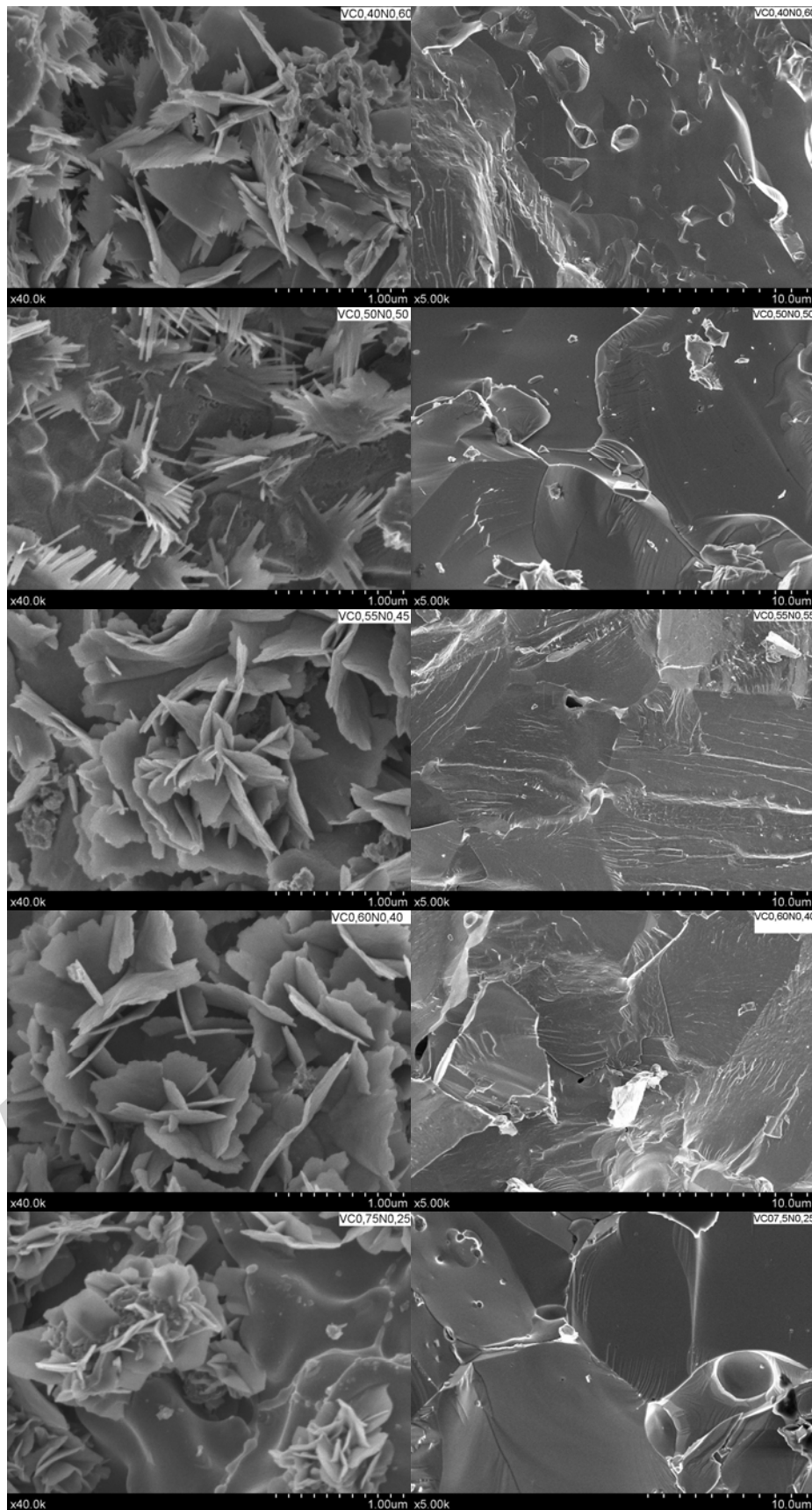
Sample	Mechanism	Densification (%)	Microhardness (Hv)
VC _{0.25} N _{0.75}	Difusion	88	1434
VC _{0.30} N _{0.70}	Combustion	97	1530
VC _{0.40} N _{0.60}	Combustion	94	1520
VC _{0.50} N _{0.50}	Combustion	89	1617
VC _{0.55} N _{0.45}	Combustion	91	1528
VC _{0.60} N _{0.40}	Combustion	93	1530
VC _{0.75} N _{0.25}	Combustion	92	1554
VC _{0.85} N _{0.15}	Combustion	88	1525
VC _{0.95} N _{0.05}	Combustion	89	1565

The data in Table III show a relatively good densification for the different samples. The composition VC_{0.25}N_{0.75} has the lowest microhardness and density values, which is in agreement with the results of Mittere⁴⁴, showing that an increase in the amorphous carbon phase fraction results in a reduction in hardness. Furthermore, the microhardness values are higher than those obtained for vanadium nitride and lower than those for vanadium carbide and increase as the percentage of carbon increases, which is in good agreement with Grigore⁴⁵. The highest value corresponds to the composition VC_{0.5}N_{0.5}, and this composition has, according to the calculated lattice parameter, the best stoichiometric characteristics. This behavior was previously observed by Yeh et al.¹⁴ in a study of vanadium carbonitride obtained using SHS methods and by some other authors⁴⁶⁻⁴⁷, who found a direct relationship between the microhardness for ternary nitrides (Ti, Zr)N and (Ti, Al)N and VN, in which the greater

the percentage of nitrogen and the closer the compound is to being stoichiometric, the higher the hardness. Moreover, we only have microhardness data from samples supported on steel layers; the highest microhardness value was observed by Aghaie et al.¹⁰ (2200 Hv) in a sample prepared by soaking with a gradient of carbonitride, carbide and vanadium nitride. Our value is not considerably different than this value, and the microhardness values of the bulk samples are lower than those of the films⁴⁸⁻⁴⁹.

To complete the characterization of the samples, their morphologies were investigated using scanning electron microscopy. The SEM observations were performed on a transverse view of broken tablets to avoid surface phenomena. Fig. 5 presents the microphotographs for the different compositions, and a large percentage of sintering can be observed in all samples; the high densification observed suggests that the microstructure that developed in the ground powder promotes the cold welding of the particles, which exhibit compactness close to full density. The composition with the least carbon content exhibits some imperfections and porosity, which is consistent with the obtained microhardness and density values.





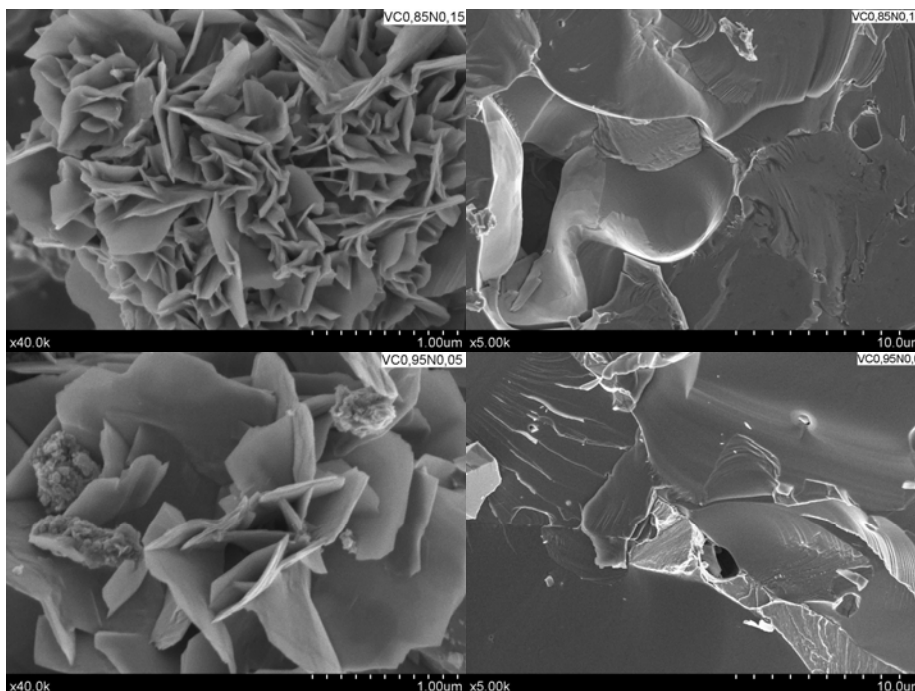


Fig. 5. Micrographs of VC_xN_{1-x} before and after sintering.

In summary, we can conclude that reactive milling is a good method for obtaining these types of compounds: it is possible to obtain all composition ranges; the procedure is inexpensive, is performed at room temperature, and requires only short synthesis times; and particles are obtained with high sinterability, very high microhardness and low contamination.

Acknowledgment

This work was supported by the Spanish government under Grant No. MAT2011-22981, which was financed in part by the European Regional Development Fund of 2007–2013.

References

1. Zalite I, Ordanyan S, Korb G. Synthesis of transition metal nitride/carbonitride nanopowders and their application for modification of structure of hardmetals. *Powder Metallurgy* 2003;46(2):143-147.
2. Baker T.N. Process, microstructure and properties of vanadium microalloyed steels. *Materials Science Technology* 2009; 25(9): 1083-1107.
3. Chicco B, Borbidge W.E, Summerville E. Experimental study of vanadium carbide and carbonitride coatings. *Mater. Sci. Eng. A* 1999; 266:62–72.
4. Valade L, Danjoy C, Chansou B, Riviere E, Pellegatta J.L, Choukroun R, Cassoux P. Evaluation of the simultaneous use of Cp_2VMe_2 and $CpTiCl_2N(SiMe_3)_2$ as

- precursors to ceramic thin films containing titanium and vanadium: Towards titanium-vanadium carbonitride. *App. Organ. Chem.* 1998; 12(3):173-187.
5. Bonnefond P, Feurer R, Reynes A, Maury F, Chansou B, Choukroun R, Cassoux P. Thermal decomposition of $V(\text{Net}_2)_4$ in an MOCVD reactor; a low-temperature route to vanadium carbonitride coatings. *J. Mat. Chem.* 1996; 6(9): 1501-1506.
 6. Laurent F, Michel P, Feurer R, Morancho R, Valade L, Choukroun R, Cassoux P. New organometallic route to vanadium carbonitride thin films. *J. Mat. Chem.* 1993; 3(6): 659-663.
 7. Poirier L, Richard O, Ducarroir M, Nadal M, Teyssandier F, Laurent F, Cyr-Athis O, Choukroun R, Valade L, Cassoux P. Vanadocene used as a precursor for the chemical-vapor-deposition of vanadium carbide at atmospheric-pressure. *Thin Solid Films* 1994; 249:62-69.
 8. Abisset S, Maury F, Pelletier I, Carretas J.M, Pires de Matos A. Depot chimique en phase vapeur a basse temperature de revetements dans le systeme V-C-N a partir de bis(arene)vanadium. *Ann.Chim.Mat.* 1998; 23:695-706.
 9. Yunchao M, Baoyan L. Combustion synthesis of $V(\text{CN})$ powders. *Advanced materials research* 2012; 452-453: 278-281.
 10. Aghaie-Khafri M, Fazlalipour F. Kinetics of $V(\text{C,N})$ coating produced by a duplex surface treatment. *Surface & interface Technology* 2008; 202:4107-4113.
 11. Spear K.E, Leitnaker J. Formation of active carbon in twin-crucible studies of vanadium carbonitride solutions. *J.Am.Ceram.Soc.* 1969; 52(5):257-262.
 12. Lumbreras J.A, Núñez G.A, Sandoval ,Melo J.A, Robles S, Garcia Alamilla. Synthesis and characterization of vanadium nitrides and carbides *Rev.Int.Contam.Ambient.* 2008; 24(1): 13-19.
 13. Preiss H, Schultze D, Szulzewsky K. Carbothermal synthesis of vanadium and chromium carbides from solution-derived precursors. *J.Eur.Ceram.Soc.* 1999;19: 187-194.
 14. Yeh C.L, Chen Y.D. Combustion synthesis of vanadium carbonitride from V-C powder compacts under nitrogen pressure. *Cer. Int.* 2007; 33:365-371.
 15. Merzhanov A.G. Solid flames-discoveries, concepts and horizons of cognition. *Combust. Sci. Technol.* 1994; 98(4-6): 307-336.
 16. Moore J.J, Feng H.J. Combustion synthesis of advanced materials 1. Reaction parameters. *Progr. Mater. Sci.* 1995; 39(4-5):243-273.
 17. Mossino P. Some aspects in self-propagating high-temperature synthesis. *Ceram. Int.* 2004; 30(3):311-332.

18. Anselmi-Tamburini U, Munir Z.A. The propagation of a solid-state combustion wave in Ni-Al solids. *J. Appl. Physics* 1989; 66(10): 5039-5045.
19. Holt J.B, Munir Z.A. Combustion synthesis of titanium carbide- theory and experiment. *J. Mater. Sci.* 1986; 21(1): 251–2599.
20. Kim T, Wooldridge M.S. Catalytically assisted self-propagating high-temperature synthesis of tantalum carbide powders. *J. Am. Ceram. Soc.* 2001; 84 (5): 976–982.
21. Eslamloo-Grami M, Munir Z.A. Effect of porosity on the combustion synthesis of titanium nitride. *J. Am. Ceram. Soc.* 1990; 73(5):1235–1239.
22. Agrafiotis C.C, Puszynski J.A, Hlavacek V. Experimental-study on the synthesis of titanium and tantalum nitrides in the self-propagating regime. *Combust. Sci. Technol.* 1991; 76(4-6): 187–218.
23. Eslamloo-Grami M, Munir Z.A. The mechanism of the combustion synthesis of titanium carbonitride. *J. Mater. Res.* 1994; 9 (2): 431–435.
24. Khyzhun O.Y, Kolyagin V.A. Electronic structure of cubic and rhombohedral tantalum carbonitrides studied by XPS, XES and XAS methods. *J. Electron Spectrosc. Related Phenomena* 2004; 137–140: 463–467.
25. Speer J.G, Mehta S, Hansen S.S. Composition of vanadium carbonitride precipitates in microalloyed austenite. *Scrip. Met.* 1984; 18 (11): 1241-1244.
26. Córdoba J.M, Sayagués M.J, Alcalá M.D, Gotor F.J. Monophasic $Ti_yNb_{1-y}C_xN_{1-x}$ nanopowders obtained at room temperature by MSR. *J.Mater.Chem.* 2007; 17:650-653.
27. Córdoba J.M, Sayagués M.J, Alcalá M.D, Gotor F.J. Monophasic nanostructured powders of niobium, tantalum and hafnium carbonitrides synthesis by a mechanically induced self-propagating reaction. *J.Am.Ceram.Soc.* 2007; 90(2): 381-387.
28. Roldán M.A, Alcalá M.D, Real C. Characterisation of ternary $Ti_xV_{1-x}N_y$ nitride prepared by mechanosynthesis. *Ceramics International* 2012; 38(1): 687–693.
29. Yeh C.L, Liu E.W. Preparation of tantalum carbonitride by self-propagating high-temperature synthesis of Ta-C system in nitrogen. *Ceram. Int.* 2006; 32(6):653–658.
30. Matteazzi P, Le Caer G. Room-temperature mechanosynthesis of carbides by grinding of elemental powders. *J.Am.Ceram.Soc.* 1991; 74(6): 1382-1390.
31. Calka A, Kaczmarek W.A. The effect of milling condition on the formation of nanostructures: synthesis of vanadium carbides. *Scripta Metal.Mater.* 1992; 26: 249-253.

32. Zhang B, Li, Z.Q. Synthesis of vanadium carbide by mechanical alloying. *J. Alloys Comp.* 2005; 392:183-186.
33. Yen B.K, Aizawa T, Kihara J. Synthesis and formation mechanisms of molybdenum silicides by mechanical alloying. *Mater. Sci. Eng. A* 1996; 220(1-2):8-14.
34. Munir Z. A. Synthesis of high-temperature materials by self-propagating combustion methods. *American Ceramic Bulletin* 1988; 67 (2): 342-349.
35. Anselmi-Tamburini U, Maglia F, Doppio S, Monagheddu A, Cocco G, Munir Z.A. Ignition mechanism of mechanically activated Me-Si (Me= Ti, Nb, Mo) mixtures. *J. Mater. Res.*, 2004; 19(5):1558-1565.
36. Takacs L. Ball mill-induced combustion in powder mixtures containing titanium, zirconium or hafnium. *J. Solid State Chem.* 1996; 125(1):75-84.
37. Liu Z.G, Guo J.T, Hu H.Q. Mechanical alloying of the Ni-Al(M) (M=Ti,Fe) system. *Mater. Sci. Eng. A* 1995; 192: 577-582.
38. Yeh C.L., Chen Y.D. Direct formation of titanium carbonitrides by SHS in nitrogen. *Ceram. In.* 2005; 31(5):719-729.
39. Yeh C.L., Chen Y.D. Synthesis of niobium carbonitrides by self-propagating combustion of Nb-C system in nitrogen. *Ceram. In.* 2005; 31(8):1031-1039.
40. Yeh C.L., Liu E.W. Preparation of tantalum carbonitrides by self-propagating high-temperature synthesis of Ta-C system in nitrogen. *Ceram. In.* 2006; 32(6):653-658.
41. Lichtenberger O, Pippel E, Woltersdorf J, Riedel R. Formation of nanocrystalline titanium carbonitride by pyrolysis of poly(titanycarbodiimide). *Mater. Chem. Phys.* 2003; 81(1):195-201.
42. Martinez-Martinez D, Sánchez-López J.C, Rojas T.C, Fernandez A, Eaton P, Belin M. Structural and microtribological studies of Ti-C-N based nanocomposite coating prepared by reactive sputtering. *Thin Solid Films* 2005; 472:64-70.
43. Sánchez-López J.C, Donnet C, Belin M, Le Mogne T, Fernandez-Ramos C, Sayagues M.J, Fernandez A. Tribochemical effects on CN_x films. *Surf. & Coat. Technol.* 2000; 133-134: 430-436.
44. Mitterer C, Fateh N, Munnik F. Microstructure-property relations of reactively magnetron sputtered VC_xNy films. *Surface and Coating Technology* 2011; 205: 3805-3809.
45. Grigore E, Ruset C, Li X, Dong H. The influence of carbon content on the characteristics of V-C-N coatings deposited by combined magnetron sputtering and ion implantation (CMSII). *Surface and Coating Technology* 2010; 204:2006-2009.

46. Sanjinés R, Wiemer C, Hones P, Lévy F. Chemical bonding and electronic structure in binary VNy and ternary Ti_{1-x}VxNy nitrides. *J.App. Phys* 1998; 83(3): 1396-1402.
47. Toth L.E. In transition metal carbides and nitrides, Academic Press, New York 1971; vol.7.
48. Sundgren J.E, Hentzell H.T.G. A review of the present state of art in hard coatings grown from the vapour-phase. *J.Vac.Sci.Technol.A* 1986; 4(5): 2259-2279.
49. Hones P, Sanjines R, Levy F, Shojaei O. Electronic structure and mechanical properties of resistant coatings: The chromium molybdenum nitride system. *J.Vac.Sci.Technol.A* 1999; 17(3): 1024-1030.

Accepted manuscript